Int J Clin Exp Pathol 2015;8(4):3681-3690
www.ijcep.com /ISSN:1936-2625/IJCEP0006127

*Original Article*

# Ursolic acid derivative ameliorates streptozotocin-induced diabestic bone deleterious effects in mice

Su-Guo Yu[1], Cheng-Jie Zhang[2], Xiu-E Xu[3], Ji-Hua Sun[1], Li Zhang[1], Peng-Fei Yu[1]

*[1]Department of Endocrinology, Affiliated Hosptial of Binzhou Medical University, Binzhou 256603, China; [2]Department of Emergency, People's Hospital of Binzhou, Binzhou 256610, China; [3]Department of Endocrinology, Hospital of Yangxin Traditional Chinese Medicine, Binzhou 251880, China*

Received January 19, 2015; Accepted March 20, 2015; Epub April 1, 2015; Published April 15, 2015

**Abstract:** Objective: This study was performed to investigate bone deteriorations of diabetic mice in response to the treatment of ursolic acid derivative (UAD). Methods: The biomarkers in serum and urine were measured, tibias were taken for the measurement on gene and protein expression and histomorphology analysis, and femurs were taken for the measurement on bone Ca and three-dimensional architecture of trabecular bone. Results: UAD showed a greater increase in bone Ca, BMD and significantly increased FGF-23 and OCN, reduced PTH and CTX in diabetic mice. UAD reversed STZ-induced trabecular deleterious effects and stimulated bone remodeling. The treatment of STZ group with UAD significantly elevated the ratio of OPG/RANKL. Moreover, insulin and IGF-1 showed a negative correlation with both FBG and Hb1Ac in STZ group. We attributed down-regulating the level of Hb1Ac in diabetic mice to that ursolic acid derivative could primely control blood sugar levels. After analyzing of two adipocyte markers, PPARγ and aP2, increased expression in the tibias of diabetic mice, and UAD could improve STZ-induced adipocyte dysfunction. Conclusions: These results demonstrated that UAD could ameliorate STZ-induced bone deterioration through improving adipocyte dysfunction and enhancing new bone formation and inhibiting absorptive function of osteoclast in the bone of diabetic mice.

**Keywords:** OPG/RANKL, PPARγ, diabetic, ursolic acid derivative, bone

## Introduction

Type 1 diabetes mellitus (DM1) results in hyperglycemia because of an absolute insulin insufficiency. This leads to many complications, both microvascular and macrovascular pathological changes [1], retinopathy [2, 3], neuropathy [4], diabetic nephropathy [5], diabetic osteopenia and osteoporosis [6]. Recent clinical surveys showed that DM1 elevates fracture risks of hip, vertebral, proximal humerus, tibia, wrist and ankle independent of BMD [7, 8]. Moreover, DM1 has been recognized a relationship between delayed healing of fractures and bone defects in animal models [9, 10]. Osteoporosis is one of the long-term complications associated with DM1. The well-known causes for diabetic osteoporosis include the direct effects of insulin deficiency or resistance and hyperglycemia on bone and the bone marrow microenvironment. The duration of DM1, microvascular complications may account for low bone mass and increased fracture risk. Additionally, advanced glycation end-products of bone matrix proteins, and some biological factors like cytokines and adipokines, could exert their detrimental effects on bone cells [11].

Osteoblasts are originated from mesenchymal stem cells, which can differentiate into adipocytes as well as a variety of other cell types [6]. During the process of osteogenesis and osteoblast differentiation, Runx2, a transcription factor, and TGF-β are markedly elevated [12]. Subsequent overexpression bone formation marker genes, such as osteocalcin (OCN), alkaline phosphatase (ALP), type I collage (COL I), were demonstrated during osteogenetic process in vitro [12]. On the other hand, overexpression of peroxisome proliferator activated receptor γ (PPARγ), a member of the nuclear receptor transcription factor family, induces adipogenesis over osteoblastogenesis in mcsenchymal stem cells (MSCs) [13-15].

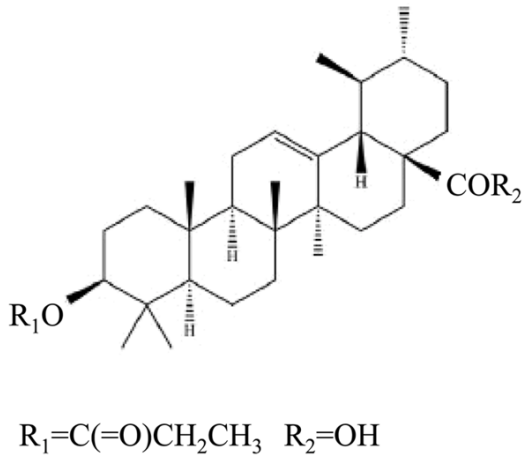


**Figure 1.** The structure of ursolic acid derivative.

Interestingly, inhibition of PPAR-γ during induction of osteogenesis leads to increased osteogenic differentiation of human MSCs [14]. Selection of adipogenesis over osteoblastogenesis is thought to contribute to bone loss associated with a variety of conditions including senescence [16], estrogen deficiency [17] and hyperglycemia [6].

Bone deteriorations induced by hyperglycemia is mediated, at least partially, through the OPG/RANKL system, which can influence the local metabolism environment of bone and play an important role of regulating osteoclast differentiation and activity [18]. Osteoclastogenesis depends on osteoblasts secreting the key mediator, receptor activator of nuclear factor-kB (RANK) ligand (RANKL), which binds to its receptor (RANK) on the plasma membrane of osteoclast precursors, thereby stimulating differentiation of pre-osteoclasts into mature osteoclasts. Moreover, to counterbalance RANKL action, osteoblasts synthesize and secrete osteoprotegerin (OPG), a soluble decoy receptor capable of inhibiting RANK-RANKL interaction and osteoclastogenesis [19]. Recent clinical data indicates that OPG mRNA expression and plasma OPG levels are significantly increased in DM1 groups in comparison with NG group. Children and adolescents with early onset DM1 present low bone mineral density, associated to unsatisfactory glycemic control, increased OPG levels and low osteocalcin concentration [7, 20].

Ursolic acid is a pentacyclic triterpene, which is abundantly distributed in medicinal herbs. Pharmacological effects of ursolic acid include anti-cancer [21], anti-inflammatory [22], anti-viral [23], anti-diabetic activities [24], stimulating osteoblast differentiation and enhancing new bone formation [25] and so on. Recent approaches in the early stage of drug discovery and development include the development of therapeutic agents from natural substances, which retain the beneficial effects while minimizing the adverse side effects, but effects of ursolic acid on diabetic osteoporosis have not been determined. Therefore, here we used a streptozotocin-induced diabetic mouse model to examine the effect of ursolic acid on bone. Bone metabolism key regulators and adipocyte markers, PPARγ and aP2, were detected.

## Materials and methods

### *Animal treatment*

Six-week-old male C57BL/6J mice (Slac Laboratory Animal, Shanghai, China) were allowed to acclimate to the environment for 1 week. All experimental procedures were carried out in accordance with the guidelines of The Affiliated Hosptial of Binzhou Medical University on Animal Care. Ursolic acid derivatives (UAD, **Figure 1**) were obtained from our research team. These compounds were purified by column chromatography and their structures were all confirmed. All chemicals and reagents were purchased from Sigma (Oakville, Ontario, Canada), except where noted.

The mice were randomly divided into three groups: (1) Vehicle group (n = 12); (2) Streptozotocin (STZ)-induced hyperglycemia mice (DM1, n = 12); (3) STZ with ursolic acid-treated group received ursolic acid orally at a dose of 200 mg/kg per day (US, n = 12). The mice were induced hyperglycemia by intraperitoneal injection of STZ, dissolved in citrate buffer (0.1 M at pH 4.2), at 35 mg/kg body weight for 5 consecutive days. The mice in vehicle group were injected with solvent. All mice were sacrificed 6 weeks after STZ injection. The fasting blood glucose (FBG) levels were measured with a blood glucose monitoring system (Roche). Body weight and FBG were recorded every two weeks during experimental period.

### *Bone metablism key regulators and calcium in serum, urine and bone*

The concentrations of calcium (Ca) from serum and urine were measured by standard colori-

**Table 1.** Primers sequence used for RT-PCR analysis

| gene | Forward primer sequence (5'-3') | Reverse primer sequence (5'-3') |
|---|---|---|
| RANKL | tcaggagttccagctatgat | ccatcagctgaagatagtcc |
| OPG | tcactgggctgtttcttcag | tcctctttctcagggtgctt |
| MMP-9 | ggtcggttctgacctttgt | tggtgtcctccgatgtaaga |
| CAII | tggttcactggaacaccaaa | agcaagggtcgaagttagca |
| TGF-β | tgacgtcactggagttgtacgg | ggttcatgtcatgatggtgc |
| Runx2 | tcaacatccgccaagagg | tacttgatgccacctgcgatg |
| PPARγ | gcgcagggaacaagcagagc | gccctcgagcggaagactgtg |
| aP2 | cacgtccacaactagaaggtgg | gaccaacgaatcgtagcctgg |
| GAPGH | gtgaggtgaccgcatcttct | cttgccgtgggtagagtcat |

metric methods using a micro-plate reader (Bio-Tek, USA). The level of urine Ca was corrected by the concentration of creatinine (Cre). Serum levels of intact parathyroid hormone (PTH 1-84), fibroblast growth factor-23 (FGF-23), tartrate resistant acid phosphatase-5b (TRACP-5b), osteocalcin (OCN), C-terminal telopeptide of type I collagen (CTX), testosterone (TES) and bone specific alkaline phosphatase (b-ALP) were detected using mouse bioactive PTH ELISA assay (Santa Cruz Biotechnology, Santa Cruz, CA, USA) with ELISA reader (MD SpectraMax M5, USA).

The tibias were incinerated at 800°C for 6 hours and the ash weighed. 10 mg of bone ash was then dissolved in 1 ml of 37% HCl and diluted with Millin-Q water. The calcium content was determined by the kit used for serum and urine calcium assay.

*Bone histomorphology*

The tibias were decalcified in 0.5 M EDTA (pH = 8.0) and then embedded in paraffin by standard histological procedures. Section of 5 μm were cut and stained with hematoxylin & eosin (H&E), and visualized under a microscope (Leica DM 2500).

The trabecular bone microarchitecture of the proximal metaphysis of the tibia was measured using a microtomography scanner (SkyScan 1076, Kontizh, Belgium) with a slice thickness of 22 μm. The volume of interest (VOI) was trabecular compartments based on 100 consecutive slices away from the proxomal tibia growth plate. The 3D images were obtained for visualization and display. Bone morphometric parameters, including bone volume over total volume (BV/TV), trabecula number (Tb. N), trabecula thickness (Tb. Th) and bone mineral density over total volume (BMD/TV) were obtained by analyzing the VOI.

*Reverse transcription-polymerase chain reaction*

The tibias of each animal were crushed under liquid nitrogen conditions and RNA extraction was performed according to the TRIzol manufacturer's protocol (Invitrogen, Carlsbad, CA, USA). RNA integrity was verified by agarose gel electrophoresis. Synthesis of cDNAs was performed by reverse transcription reactions with 2 μg of total RNA using moloney murine leukemia virus reverse transcriptase (Invitrogen) with oligo dT (15) primers (Fermentas) as described by the manufacturer. The first strand cDNAs served as the template for the regular polymerase chain reaction (PCR) performed using a DNA Engine (ABI 7300). Glyceraldehyde 3-phosphate dehydrogenase (GAPDH) as an internal control was used to normalize the data to determine the relative expression of the target genes. The reaction conditions were set according to the kit instructions. The PCR primers used in this study were shown in **Table 1**.

*Statistical analysis*

The data from these experiments were reported as mean ± standard error of mean (SEM) for each group. All statistical analyses were performed using PRISM version 4.0 (GraphPad). Inter-group differences were analyzed by one-way ANOVA, and followed by Tukey's multiple comparison test as a post test to compare the group means if overall $P < 0.05$. Differences with $P$ value of < 0.05 were considered statistically significant.

## Results

*Physiological and biochemical properties*

Two weeks after the STZ injection, fasting blood glucose (FBG) was measured, and whole blood was collected from the orbital vein to confirm diabetes at levels greater than 11.1 mmol/L. The FBG value of DM1 mice rose from 11.2 mmol/L at week 2 to 17.4 mmol/L at week 6. The FBG in the DM1 group was significantly

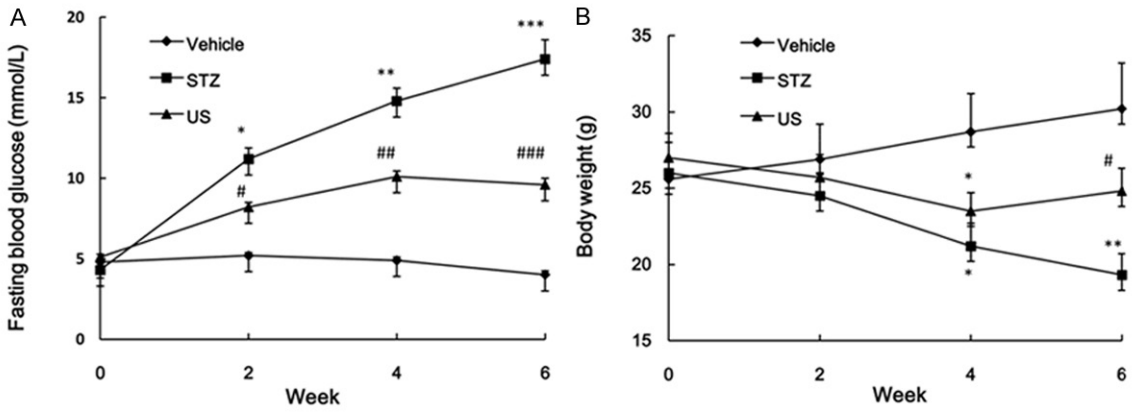


**Figure 2.** Body weight (BW) and fasting blood glucose (FBG) throughout the study. BW (A) and FBG (B) are recorded every two weeks during experimental period. Values are expressed as mean ± SEM, n = 12 in each group. $^{*}P < 0.05$, $^{**}P < 0.01$, $^{***}P < 0.001$, versus vehicle group; $^{\#}P < 0.05$, $^{\#\#}P < 0.01$, $^{\#\#\#}P < 0.001$, versus STZ group.

**Table 2.** Calcium content in serum, urine and bone

| | Vehicle | STZ | US |
|---|---|---|---|
| Ca/Ash (mg/mg) | 0.47 ± 0.028 | 0.22 ± 0.019* | 0.39 ± 0.022# |
| Bone Ca (mg) | 8.5 ± 0.38 | 4.5 ± 0.45* | 7.0 ± 0.30# |
| Serum Ca (mg/dL) | 10.65 ± 0.31 | 9.05 ± 0.32* | 10.07 ± 0.38# |
| Urine Ca/Cre (mg/mg) | 0.039 ± 0.004 | 0.084 ± 0.009* | 0.055 ± 0.007# |

Values are expressed as mean ± SEM, n = 6 in each group. $^{*}P < 0.05$, versus vehicle group; $^{\#}P < 0.05$, versus STZ group.

**Table 3.** Bone parameters of proximal tibia

| | Vehicle | STZ | US |
|---|---|---|---|
| BV/TV (%) | 37 ± 3.6 | 19 ± 2.4* | 28 ± 3.2# |
| Tb. N ($mm^{-1}$) | 8.8 ± 0.72 | 5.1 ± 0.32* | 7.9 ± 0.90# |
| Tb. Th (μm) | 52 ± 4.3 | 27 ± 4.0* | 50 ± 4.5# |
| BMD/TV (mg HA/$cm^3$) | 150 ± 12.2 | 78 ± 10.6* | 109 ± 13.3# |

BV/TV, bone volume over total volume; Tb. N, trabecula number; Tb. Th, trabecula thickness; BMD/TV, bone mineral density over total volume. Values are expressed as mean ± SEM, n = 6 in each group. $^{*}P < 0.05$, versus vehicle group; $^{\#}P < 0.05$, versus STZ group.

increased compared to that of the control group from week 2 to week 6 (**Figure 2A**). At the end of the 6 week treatment, 200 mg/kg of UAD decreased FBG (44.8%) as compared with diabetic control. The mean body weight (BW) of the STZ-treated mice was significantly lower than that of the control group (**Figure 2B**). In contrast, BW of diabetic mice was increased after week 4 of the UAD treatment.

The Ca level in serum, urine and bone was comparable in the three experimental groups. Hyperglycemia could up-regulate urine Ca excretion and down-regulate the Ca content in bone and serum (**Table 2**). STZ-treated could accelerate calcium outflow. When comparing the results of serum, urine and bone between STZ and US groups, we could easily see that the UAD increased serum Ca, decreased urine Ca excretion and increased bone calcium content (**Table 2**). From these calcium metabolic data, it was well shown that UAD exerted protective effects on maintaining calcium balance of STZ-induced bone deteriorations in mice.

*Micro-CT and bone histology*

The loss of trabecular bone mass at the proximal metaphysis of the tibia was quantified using micro-CT scanning. Analyses of the data from the proximal metaphysis of the tibia revealed that diabetic mice exhibited significantly lower trabecular BMD/TV, BV/TV, Tb. N and Tb. Th, compared to that of the control group (**Table 3**). Notably, treatment with UAD for diabetic mice resulted in increasing the BV/TV ratio, Tb. N, Tb. Th and BMD/TV (**Table 3**). Histological analysis on trabecular bone in proximal metaphysis of mice was performed by H&E staining (**Figure 3A**). The histology of trabecular bone below growth plate was markedly different in the three experimental groups. H&E staining showed the increased disconnections and separation among growth

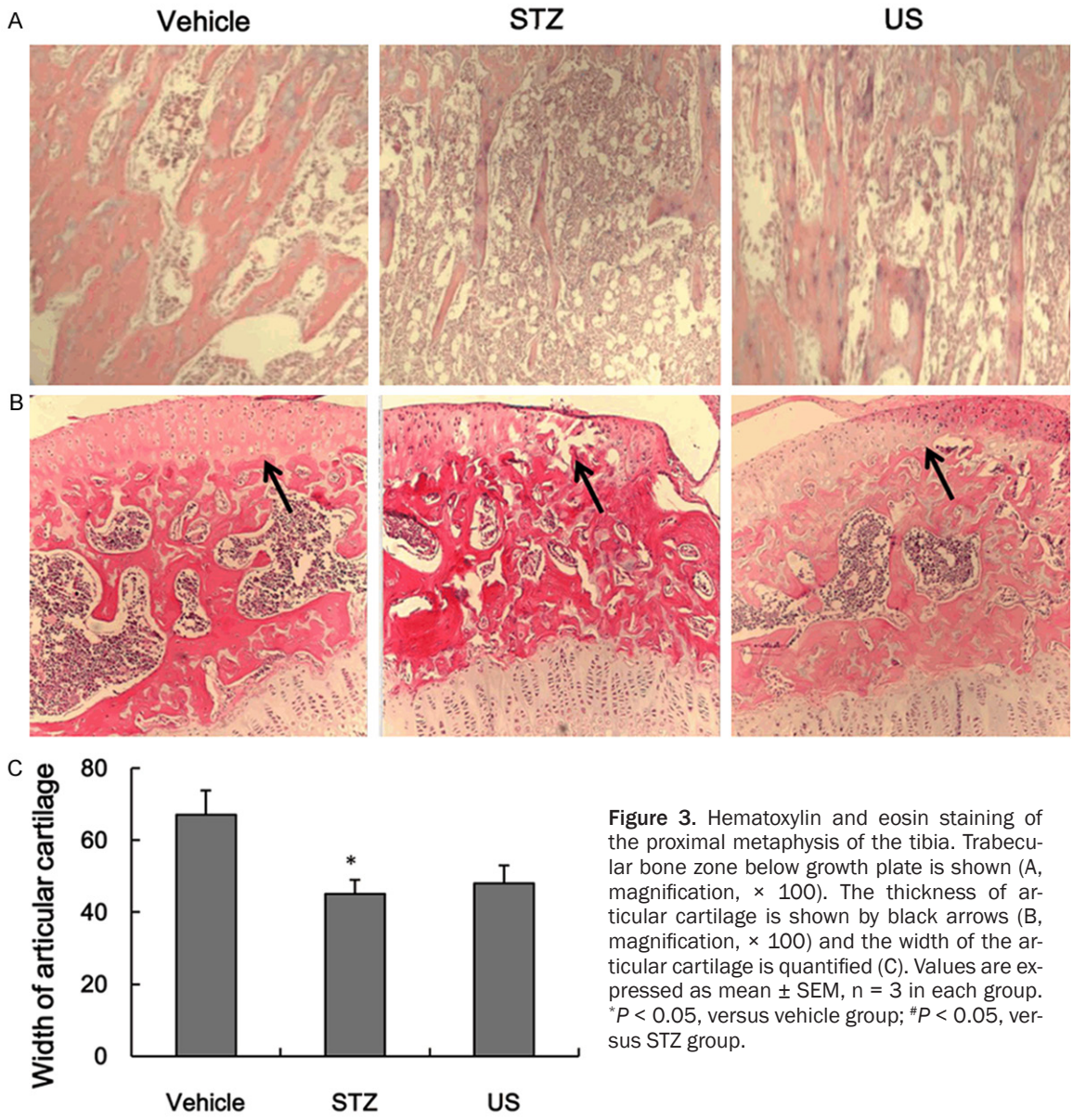


**Figure 3.** Hematoxylin and eosin staining of the proximal metaphysis of the tibia. Trabecular bone zone below growth plate is shown (A, magnification, × 100). The thickness of articular cartilage is shown by black arrows (B, magnification, × 100) and the width of the articular cartilage is quantified (C). Values are expressed as mean ± SEM, n = 3 in each group. $^{*}P < 0.05$, versus vehicle group; $^{\#}P < 0.05$, versus STZ group.

plate and trabecular bone network as well as the reduction of trabecular bone mass of primary and secondary spongiosa throughout the proximal metaphysis of tibia in STZ group. Importantly, UAD reversed STZ-induced trabecular deleterious effects and stimulated bone remodeling (**Figure 3A**). Moreover, H&E staining was performed to observe the articular cartilage at the proximal metaphysis of the tibia. The thickness of articular cartilage was reduced in the proximal tibia of STZ group (**Figure 3B** and **3C**). The black arrow indicated that articular cartilage suffered seriously injured, so not in its integrity. UAD reversed STZ-induced articular cartilage damage and maintained integrity of articular cartilage in the proximal tibia (**Figure 3B** and **3C**).

*Bone metabolic biochemical makers*

Serum concentrations of bone turnover markers, like TRACP-5b as a bone resorption marker and b-ALP as a bone formation marker, were determined. The results showed that the serum PTH and CTX level in STZ group were significantly increased, and the serum FGF-23, OCN, TES and b-ALP level were significantly decreased when compared to that of the control group (**Table 4**). The serum PTH, TRACP-5b and CTX level in US group were lower than STZ

**Table 4.** Bone metabolism-related biochemical markers in serum

| | Sham | STZ | US |
|---|---|---|---|
| Intact PTH (pg/mL) | 109 ± 5.1 | 164 ± 8.7* | 125 ± 4.2# |
| FGF-23 (pg/mL) | 385 ± 20.7 | 188 ± 16.3* | 301 ± 17.4# |
| TRACP-5b (pg/mL) | 2.75 ± 0.37 | 2.87 ± 0.49 | 2.79 ± 0.31 |
| OCN (ng/mL) | 556 ± 25.8 | 339 ± 29.9* | 476 ± 29.1# |
| CTX (ng/mL) | 37 ± 4.4 | 69 ± 5.9* | 48 ± 6.2# |
| TES (ng/mL) | 3.6 ± 0.53 | 1.2 ± 0.44* | 1.8 ± 0.45 |
| b-ALP (ng/mL) | 2.33 ± 0.05 | 1.65 ± 0.06* | 2.18 ± 0.05# |

Values are expressed as mean ± SEM, n = 6 in each group. *$P$ < 0.05, versus vehicle; #$P$ < 0.05, versus STZ. PTH, parathyroid hormone; FGF-23, fibroblast growth factor-23; TRACP-5b, tartrate resistant acid phosphatase-5b; OCN, osteocalcin; CTX, C-terminal telopeptide of type I collagen; TES, testosterone; b-ALP, bone specific alkaline phosphatase.

group, and the serum FGF-23, OCN and b-ALP level were significantly elevated in US group (**Table 4**). Inhibition streptozotocin-induced bone deleterious effects of UAD was observed in the proximal tibia suggesting that it might derive from the activity of ursolic acid to stimulate osteoblast differentiation and mineralization and suppress absorptive function of osteoclast.

*Metabolic properties and adipocyte markers in mice*

In diabetic mice, the serum insulin, IGF-1 and leptin level were significantly decreased, and ursolic acid could correct the concurrent deficiencies of insulin, IGF-1 and leptin in diabetic mice (**Figure 4A-C**). Insulin and IGF-1 showed a negative correlation with both FBG and Hb1Ac in STZ group (**Figures 2A** and **4D**). We attributed down-regulating the level of Hb1Ac in diabetic mice to that UAD could primely control blood sugar levels. Analysis of two adipocyte markers, PPARγ and aP2, demonstrated increased expression in diabetic tibia (**Figure 4E** and **4F**). These data suggested that hyperglycemia might contribute to adipocyte differentiation and proliferation in the tibia of mice. Interestingly, UAD could reverse STZ-induced mcsenchymal stem cells dysfunction.

*Osteoprotegerin/receptor activator of nuclear factor kappa B ligand (OPG/RANKL) ratio*

The maturation and formation of osteoclasts were mainly regulated by the balance of extracellular OPG and RANKL levels, thus, the ratio of OPG/RANKL expression in tibia was determined in our study. The RT-PCR result showed that the ratio of OPG/RANKL and OPG were significantly decreased, and RANKL was increased in mice treated by STZ as compared to the non-diabetic mice (**Figure 5A** and **5B**). The treatment of STZ group with UAD significantly elevated the ratio of OPG/RANKL. However, the mRNA expression of RANKL was no obvious difference in both the STZ and US group (**Figure 5A** and **5B**).

*mRNA expression of key regulators for bone metabolism*

To determine the changes of the osteoblast-specific and osteoclast-specific genes which are responsible for osteoblasts-involved bone formation and osteoclasts-involved bone resorption, the mRNA expression of runt-related transcription factor 2 (Runx2), transforming growth factor b (TGF-β), carbonic anhydrase II (CAII) and matrix metalloproteinase (MMP9) was measured. The results showed that the mRNA expression of MMP9 and CAII was significantly increased in the STZ group compared to those of non-diabetic mice (**Figure 5C** and **5D**). In contrast, the mRNA expression of Runx2 and TGF-β was significantly decreased in the STZ group compared to those of non-diabetic mice (**Figure 5C** and **5D**). UAD could simultaneously reverse the mRNA expression of MMP9, CAII, Runx2 and TGF-β in diabetic mice (**Figure 5C** and **5D**). These results suggested that UAD had the anabolic potential to stimulate osteoblast differentiation, enhance new bone formation, and suppress absorptive function of osteoclast.

## Discussion

In this study, we investigated the pharmacological roles of UAD in STZ-induced diabetic mice. UAD as a hypoglycemic agent has been applied to treatment non-obese type 2 diabetic mice. The plasma and pancreatic insulin concentrations are significantly higher in ursolic acid groups than in the untreated diabetic group [26]. Ursolic acid through absorptive and metabolic targets ameliorates abdominal adiposity and decreases the levels of blood glucose and plasma lipids in mice [27]. In KKAy with spontaneous type 2 diabetic mice, ursolic acid can ameliorate insulin resistance via improving the expression of peroxisome proliferator-activated

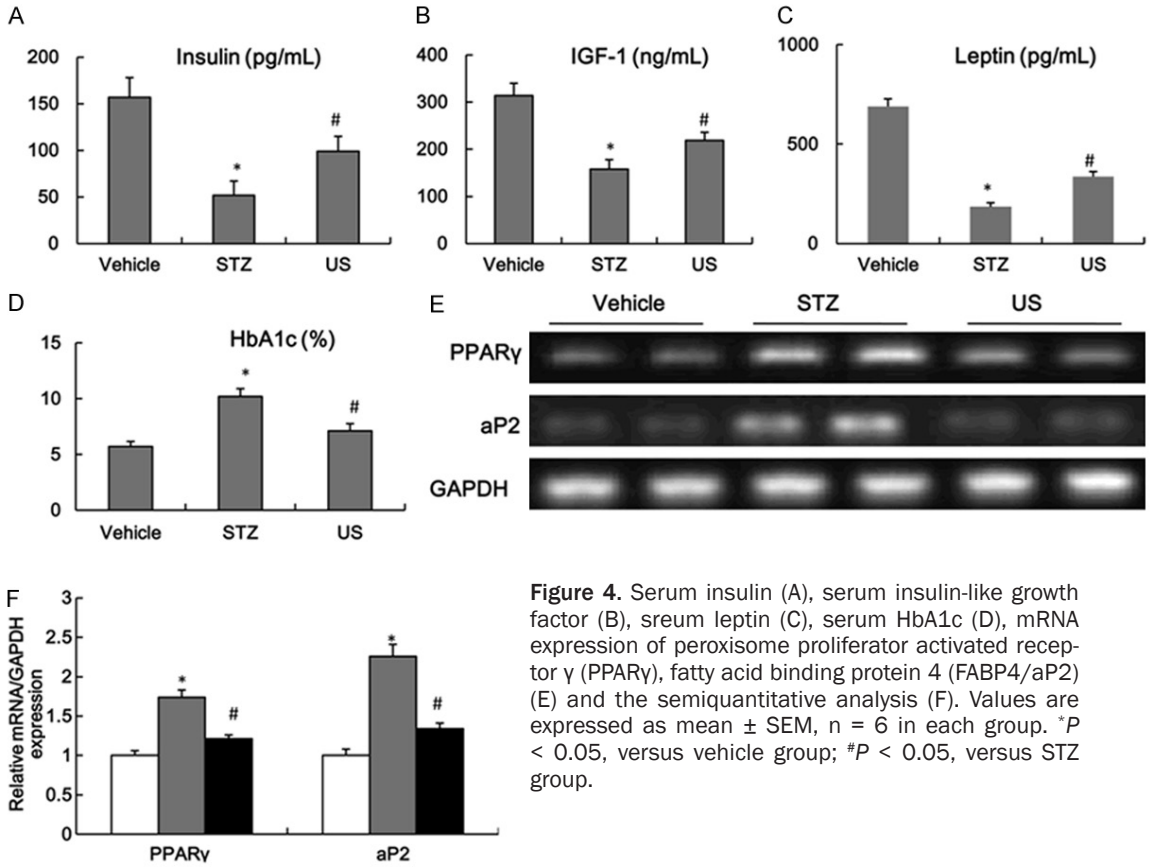


**Figure 4.** Serum insulin (A), serum insulin-like growth factor (B), sreum leptin (C), serum HbA1c (D), mRNA expression of peroxisome proliferator activated receptor γ (PPARγ), fatty acid binding protein 4 (FABP4/aP2) (E) and the semiquantitative analysis (F). Values are expressed as mean ± SEM, n = 6 in each group. $^{*}P < 0.05$, versus vehicle group; $^{\#}P < 0.05$, versus STZ group.

receptors α (PPARα) [28]. Our studies shown that ursolic acid derivatives could regulate the level of insulin, IGF-1 and Hb1Ac in the serum of diabetic mice. Insulin and IGF-1 showed a negative correlation with both FBG and Hb1Ac in STZ group. We attributed down-regulating the level of Hb1Ac in diabetic mice to that ursolic acid derivatives could primely control blood sugar levels. Moreover, we demonstrated that ursolic acid could ameliorate STZ-induced mcsenchymal stem cells dysfunction through regulation the expression of adipocyte markers PPARγ and aP2. PPARγ insufficiency results in the enhancement of osteogenesis and suppression of adipogenesis in mice, in contrast, overexpression of PPARγ levels have a dominant suppressive influence on osteogenic differentiation of human MSCs [14, 29].

We concluded that hyperglycemia increasing in bone resorption was confirmed by the increased level of PTH and CTX in the serum, and the decreased level of serum Ca and OCN and the increased level of urinary Ca excretion. Moreover, histomorphology staining also confirmed the results. A recently identified phosphatonin, known as fibroblast growth factor 23 (FGF-23), disclosed new pathways in the pathophysiology of mineral metabolism [30]. Clinical studies had shown that the downregulation of serum FGF-23 levels in Crohn disease appeared as a secondary compensatory effect on the bone and mineral metabolism induced by chronic intestinal inflammation [31]. This study provided evidence that the downregulation of serum FGF-23 levels in diabetic mice. A variety of studies have investigated the biological activity of ursolic acid *in vitro* and *in vivo*. It stimulates osteoblast differentiation and mineralization by promoting the activation of MAP kinases and transcription factors, NF-κB and AP-1 *in vitro* [25]. Moreover, ursolic acid derivatives significantly reduce hyperglycemia by increasing levels of serum insulin *in vivo* [24]. Then, when the osteoclast-specific biomarkers were suppressed, and osteoblast-specific biomarkers were elevated by ursolic acid, all the bone abnormalities were normalized approximately. These results indicated that ursolic acid derivatives could enhance bone formation and suppress bone resorption in diabetic mice. This finding might contribute to a better under-

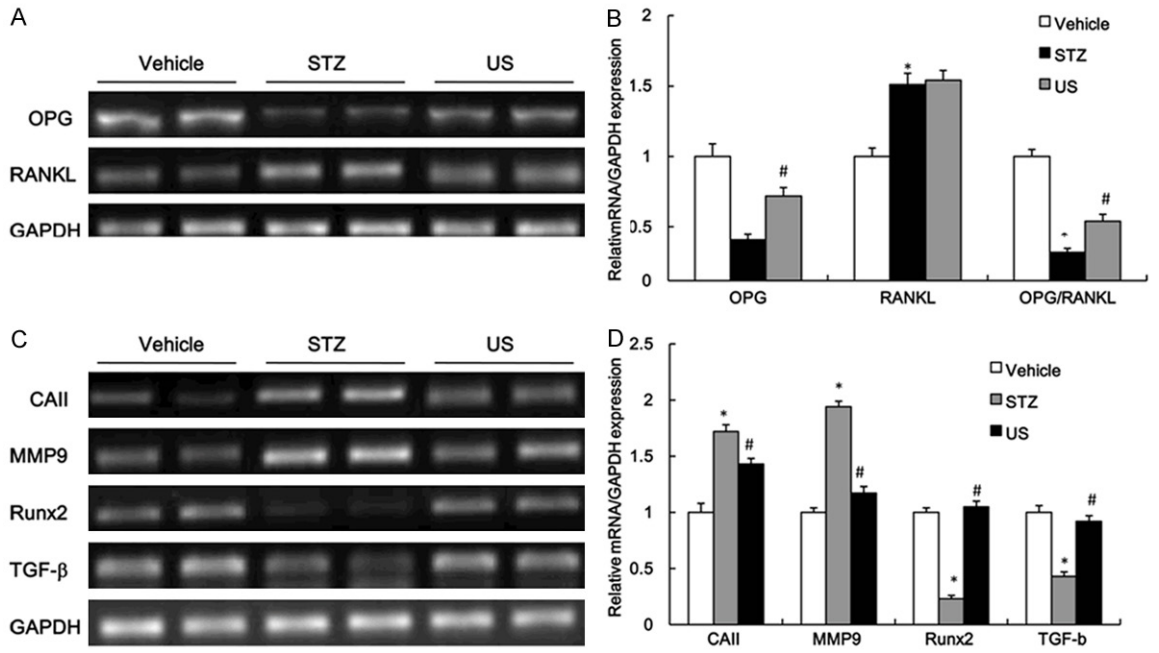


**Figure 5.** mRNA expression of osteoprotegerin (OPG), receptor activator of nuclear factor-κB ligand (RANKL) (A) and the quantitative ratio of OPG/RANKL in tibia (B). mRNA expression of runt-related transcription factor 2 (Runx2), transforming growth factor b (TGF-b), carbonic anhydrase II (CAII) and matrix metalloproteinase (MMP9) (C) and the semiquantitative analysis (D). Values are expressed as mean ± SEM, n = 6-8 in each group. $^{*}P < 0.05$, versus vehicle group; $^{\#}P < 0.05$, versus STZ group.

standing of the pharmacological roles of ursolic acid treatment diabetic osteopoorosis in mice. Thus, ursolic acid derivatives could be developed as a potentially adjuvant therapeutic or medicine prevention for diabetics mellitus and diabetic osteoporosis.

Interestingly, we demonstrated that the decreased level of testosterone in the serum of mice in STZ group. Clinical surveys showed that total osteocalcin was positively correlated with testosterone in male patients with type 2 diabetes mellitus, so total osteocalcin might predict the testosterone level in the serum [32]. In an aged orchidectomised rat model [33], testosterone replacement was able to raise the testosterone level and restore the bone volume of orchidectomised rats. We proposed that hyperglycemia may tend to suppress testosterone level and enhance bone calcium loss and collagen degradation in diabetic mice. However, ursolic acid derivatives could not improve testosterone level in diabetic mice.

According to the histomorphology staining, a decrease in the formation of new bone and articular cartilage in diabetic mice. We suspected that hyperglycemia could disequilibrate between osteoblast-osteoclast interaction and remodeling of bone in animal model. Osteoclasts were large multinucleated cells with the unique capability of extracellular resorption of the mineralized bone matrix, teeth, and mineralized cartilage [34]. The actions of osteoclasts and osteoblasts were vital for skeletal development and remodeling and the balance of bone metabolism [35]. The decreased mRNA expression ratio of OPG/RANKL in tibia indicated that hyperglycemia could stimulate osteoclastogenesis in diabetic mice. In addition, hperglycemia could increase osteoclast-involved resorptive activity as it further induced the up-regulation of MMP-9 and carbonic anhydrase II (CAII), which could act on $CO_2$ and $H_2O$ to generate the hydrogen ions that are secreted extracellularly by $H^+$-ATPase in osteoclasts to dissolve bone inorganic substance [36]. We had analyzed the mRNA expression of the osteoblast related regulators, TGF-β and Runx2, could promote osteoblastic proliferation and survival [12, 37]. This study showed that the mRNA expression of TGF-β and Runx2 in STZ group was lower than those in the control group, indicating that hyperglycemia might have direct action on suppressing osteogenic activity. Ursolic acid could simultaneously

reverse the mRNA expression of MMP9, CAII, Runx2 and TGF-β in diabetic mice. These results suggested that ursolic acid has the anabolic potential to stimulate osteoblast differentiation, enhance new bone formation, and suppress absorptive function of osteoclast.

In conclusion, we demonstrated that hyperglycemia exhibited the deterioration of trabecular bone micro-structure in mice. These alterations were mediated, at least partially, by promoting bone adiposity through up-regulation the level of PPARγ and suppressing new bone formation and enhancing absorptive function of osteoclast. Moreover, we also demonstrated that ursolic acid could ameliorate STZ-induced bone deterioration through improvement of mcsenchymal stem cells dysfunction.

## Disclosure of conflict of interest

None.

**Address correspondence to:** Dr. Su-Guo Yu, Department of Endocrinology, Affiliated Hosptial of Binzhou Medical University, No. 661 Yellow River Second Road, Binzhou 256603, China. Tel: (86)543-3256508; Fax: (86)543-3256508; E-mail: yusuguo_SD@163.com

## References

[1] Armas LA, Akhter MP, Drincic A and Recker RR. Trabecular bone histomorphometry in humans with Type 1 Diabetes Mellitus. Bone 2012; 50: 91-96.

[2] Porta M, Schellino F, Montanaro M, Baltatescu A, Borio L, Lopatina T, Trento M, Dalmasso P, Cavallo F. Prevalence of retinopathy in patients with type 1 diabetes diagnosed before and after puberty. Acta Diabetol 2014; 51: 1049-54.

[3] Shimo N, Yasuda T, Kaneto H, Katakami N, Kuroda A, Sakamoto F, Takahara M, Irie Y, Horikawa K, Miyashita K, Miyatsuka T, Yoshiuchi K, Kawamori D, Sakamoto K, Matsuoka TA, Kosugi K, Shimomura I, Matsuhisa M. Vitamin D deficiency is significantly associated with retinopathy in young Japanese type 1 diabetic patients. Diabetes Res Clin Pract 2014; 106: e41-3.

[4] Maddaloni E, Sabatino F, Del Toro R, Crugliano S, Grande S, Lauria Pantano A, Maurizi AR, Palermo A, Bonini S, Pozzilli P, Manfrini S. In vivo corneal confocal microscopy as a novel non-invasive tool to investigate cardiac autonomic neuropathy in Type 1 diabetes. Diabet Med 2015; 32: 262-6.

[5] Klein RL, Hammad SM, Baker NL, Hunt KJ, Al Gadban MM, Cleary PA, Virella G, Lopes-Virella MF; DCCT/EDIC Research Group. Decreased plasma levels of select very long chain ceramide species are associated with the development of nephropathy in type 1 diabetes. Metabolism 2014; 63: 1287-1295.

[6] Botolin S, Faugere MC, Malluche H, Orth M, Meyer R and McCabe LR. Increased bone adiposity and peroxisomal proliferator-activated receptor-gamma2 expression in type I diabetic mice. Endocrinology 2005; 146: 3622-3631.

[7] Loureiro MB, Ururahy MA, Freire-Neto FP, Oliveira GH, Duarte VM, Luchessi AD, Brandão-Neto J, Hirata RD, Hirata MH, Maciel-Neto JJ, Arrais RF, Almeida MG, Rezende AA. Low bone mineral density is associated to poor glycemic control and increased OPG expression in children and adolescents with type 1 diabetes. Diabetes Res Clin Pract 2014; 103: 452-457.

[8] Janghorbani M, Feskanich D, Willett WC and Hu F. Prospective study of diabetes and risk of hip fracture: the Nurses' Health Study. Diabetes Care 2006; 29: 1573-1578.

[9] Diao TY, Pan H, Gu SS, Chen X, Zhang FY, Wong MS, Zhang Y. Effects of angiotensin-converting enzyme inhibitor, captopril, on bone of mice with streptozotocin-induced type 1 diabetes. J Bone Miner Metab 2014; 32: 261-270.

[10] Rao Sirasanagandla S, Ranganath Pai Karkala S, Potu BK and Bhat KM. Beneficial Effect of Cissus quadrangularis Linn. on Osteopenia Associated with Streptozotocin-Induced Type 1 Diabetes Mellitus in Male Wistar Rats. Adv Pharmacol Sci 2014; 2014: 483051.

[11] Hofbauer LC, Brueck CC, Singh SK and Dobnig H. Osteoporosis in patients with diabetes mellitus. J Bone Miner Res 2007; 22: 1317-1328.

[12] Wang W, Olson D, Liang G, Franceschi RT, Li C, Wang B, Wang SS, Yang S. Collagen XXIV (Col24alpha1) promotes osteoblastic differentiation and mineralization through TGF-beta/Smads signaling pathway. Int J Biol Sci 2012; 8: 1310-1322.

[13] Shockley KR, Lazarenko OP, Czernik PJ, Rosen CJ, Churchill GA and Lecka-Czernik B. PPARgamma2 nuclear receptor controls multiple regulatory pathways of osteoblast differentiation from marrow mesenchymal stem cells. J Cell Biochem 2009; 106: 232-246.

[14] Graneli C, Karlsson C, Brisby H, Lindahl A and Thomsen P. The effects of PPAR-gamma inhibition on gene expression and the progression of induced osteogenic differentiation of human mesenchymal stem cells. Connect Tissue Res 2014; 55: 262-274.

[15] Lee MJ, Chen HT, Ho ML, Chen CH, Chuang SC, Huang SC, Fu YC, Wang GJ, Kang L, Chang JK. PPARgamma silencing enhances osteogenic differentiation of human adipose-derived mes-

enchymal stem cells. J Cell Mol Med 2013; 17: 1188-1193.
[16] Jilka RL, Weinstein RS, Takahashi K, Parfitt AM and Manolagas SC. Linkage of decreased bone mass with impaired osteoblastogenesis in a murine model of accelerated senescence. J Clin Invest 1996; 97: 1732-1740.
[17] Chen Y, Wang S, Bu S, Wang Y, Duan Y and Yang S. Treadmill training prevents bone loss by inhibition of PPARgamma expression but not promoting of Runx2 expression in ovariectomized rats. Eur J Appl Physiol 2011; 111: 1759-1767.
[18] Pater A, Sypniewska G and Pilecki O. Biochemical markers of bone cell activity in children with type 1 diabetes mellitus. J Pediatr Endocrinol Metab 2010; 23: 81-86.
[19] Zhang Z, Song C, Fu X, Liu M, Li Y, Pan J, Liu H, Wang S, Xiang L, Xiao GG, Ju D. High-dose diosgenin reduces bone loss in ovariectomized rats via attenuation of the RANKL/OPG ratio. Int J Mol Sci 2014; 15: 17130-17147.
[20] Xiang GD, Sun HL and Zhao LS. Changes of osteoprotegerin before and after insulin therapy in type 1 diabetic patients. Diabetes Res Clin Pract 2007; 76: 199-206.
[21] Rashid S, Dar BA, Majeed R, Hamid A and Bhat BA. Synthesis and biological evaluation of ursolic acid-triazolyl derivatives as potential anticancer agents. Eur J Med Chem 2013; 66: 238-245.
[22] Baricevic D, Sosa S, Della Loggia R, Tubaro A, Simonovska B, Krasna A, Zupancic A. Topical anti-inflammatory activity of Salvia officinalis L. leaves: the relevance of ursolic acid. J Ethnopharmacol 2001; 75: 125-132.
[23] Zhao J, Chen J, Liu T, Fang J, Wan J, Zhao J, Li W, Liu J, Zhao X, Chen S. Anti-viral effects of urosolic acid on guinea pig cytomegalovirus in vitro. J Huazhong Univ Sci Technolog Med Sci 2012; 32: 883-887.
[24] Wu P, He P, Zhao S, Huang T, Lu Y and Zhang K. Effects of ursolic acid derivatives on Caco-2 cells and their alleviating role in streptozocin-induced type 2 diabetic rats. Molecules 2014; 19: 12559-12576.
[25] Lee SU, Park SJ, Kwak HB, Oh J, Min YK and Kim SH. Anabolic activity of ursolic acid in bone: Stimulating osteoblast differentiation in vitro and inducing new bone formation in vivo. Pharmacol Res 2008; 58: 290-296.
[26] Lee J, Yee ST, Kim JJ, Choi MS, Kwon EY, Seo KI, Lee MK. Ursolic acid ameliorates thymic atrophy and hyperglycemia in streptozotocin-nicotinamide-induced diabetic mice. Chem Biol Interact 2010; 188: 635-642.
[27] Rao VS, de Melo CL, Queiroz MG, Lemos TL, Menezes DB, Melo TS, Santos FA. Ursolic acid, a pentacyclic triterpene from Sambucus australis, prevents abdominal adiposity in mice fed a high-fat diet. J Med Food 2011; 14: 1375-1382.
[28] Wang L, Wang GL, Liu JH, Li D, Zhu DZ and Wu LN. [Effects of ursolic acid in ameliorating insulin resistance in liver of KKAy mice via peroxisome proliferator-activated receptors alpha and gamma]. Zhong Xi Yi Jie He Xue Bao 2012; 10: 793-799.
[29] Yu WW, Xia Q, Wu Y and Bu QY. Activation of PPAR-gamma inhibits differentiation of rat osteoblasts by reducing expression of connective tissue growth factor. J Huazhong Univ Sci Technolog Med Sci 2014; 34: 652-656.
[30] Razzaque MS. The FGF23-Klotho axis: endocrine regulation of phosphate homeostasis. Nat Rev Endocrinol 2009; 5: 611-619.
[31] Oikonomou KA, Orfanidou TI, Vlychou MK, Kapsoritakis AN, Tsezou A, Malizos KN, Potamianos SP. Lower fibroblast growth factor 23 levels in young adults with Crohn disease as a possible secondary compensatory effect on the disturbance of bone and mineral metabolism. J Clin Densitom 2014; 17: 177-184.
[32] Cui R, Su B, Sheng C, Cheng X, Yang P, Bu L, Li H, Wang J, Sheng H, Qu S. Total osteocalcin in serum predicts testosterone level in male type 2 diabetes mellitus. Int J Clin Exp Med 2014; 7: 1145-1149.
[33] Tajul Ariff AS, Soelaiman IN, Pramanik J and Shuid AN. Effects of Eurycoma longifolia on Testosterone Level and Bone Structure in an Aged Orchidectomised Rat Model. Evid Based Complement Alternat Med 2012; 2012: 818072.
[34] Touaitahuata H, Cres G, de Rossi S, Vives V and Blangy A. The mineral dissolution function of osteoclasts is dispensable for hypertrophic cartilage degradation during long bone development and growth. Dev Biol 2014; 393: 57-70.
[35] Tanaka H, Tanabe N, Kawato T, Nakai K, Kariya T, Matsumoto S, Zhao N, Motohashi M, Maeno M. Nicotine affects bone resorption and suppresses the expression of cathepsin K, MMP-9 and vacuolar-type H(+)-ATPase d2 and actin organization in osteoclasts. PLoS One 2013; 8: e59402.
[36] Kartner N and Manolson MF. Novel techniques in the development of osteoporosis drug therapy: the osteoclast ruffled-border vacuolar H(+)-ATPase as an emerging target. Expert Opin Drug Discov 2014; 9: 505-522.
[37] Claros S, Rico-Llanos GA, Becerra J and Andrades JA. A novel human TGF-beta1 fusion protein in combination with rhBMP-2 increases chondro-osteogenic differentiation of bone marrow mesenchymal stem cells. Int J Mol Sci 2014; 15: 11255-11274.